crystallization communications

Crystallization and preliminary X-ray diffraction analysis of a breast cancer metastasis suppressor 1 predicted coiled-coil region

Mercedes Spínola-Amilibia, José Rivera* and Jerónimo Bravo*

Signal Transduction Group, Centro Nacional de Investigaciones Oncológicas (CNIO), Melchor Fernández Almagro 3, E-28029 Madrid, Spain

Correspondence e-mail: jrivera@cnio.es, jbravo@cnio.es

Breast cancer metastasis suppressor 1 (BRMS1) is an inhibitor of metastatic progression and plays a role in several steps of the metastatic cascade. Apart from the ability of BRMS1 to negatively regulate metastasis formation in breast, melanoma and ovarian tumours, very little is known about the molecular aspects of the antimetastatic properties of BRMS1. Here, the expression, purification and crystallization of a functional fragment of human BRMS1 that is predicted to be a coiled-coil region are reported. The purified fragment crystallized in space group $C222_1$ using the vapour-diffusion method. The unit-cell parameters were $a = 42.6$, $b = 191.3$, $c = 71.9$ Å. The crystals diffracted to 2.0 Å resolution and a complete data set was collected under cryoconditions. This is the first structural report of BRMS1.

1. Introduction

Metastasis is a life-threatening complication of cancer that represents 90% of cancer-related deaths. Metastasis takes place in several steps in which some cells detach from the primary tumour and spread, either through the lymphatic or the circulatory system, towards distant places, forming micrometastasis foci. After colonization and growth, they form secondary tumours in distant organs, developing metastasis (Gupta & Massague, 2006). Breast cancer metastasis suppressor 1 (BRMS1) is a member of a functional family of genes known as metastasis suppressors that have the ability to inhibit the appearance of macroscopic metastases without affecting the growth of the primary tumour. BRMS1 negatively regulates metastasis formation in several organs, including breast, skin (melanoma) and ovary, by acting at different steps of the metastatic cascade (Phadke *et al.*, 2008). Several *a priori* unrelated phenotypic changes such as inhibition of NFkB signalling (Cicek *et al.*, 2005), restoration of Gap-junction communications (Saunders *et al.*, 2001) or abrogation of phosphoinositide signalling (DeWald *et al.*, 2005) are induced by BRMS1.

It has been proposed that BRMS1 induces all these changes by playing a role in transcription (Liu *et al.*, 2006; Rivera *et al.*, 2007). In fact, BRMS1 can interact with several proteins that are involved in the regulation of transcription (Nikolaev *et al.*, 2004; Hurst *et al.*, 2006, 2008). BRMS1 is therefore capable of interacting with a wide range of proteins in order to promote different effects in the metastatic cascade. Human BRMS1 consists of 246 amino acids and analysis of the sequence predicts a mostly disordered protein with a few recognizable motifs, including two putative nuclear localization signals and two predicted coiled-coil regions. Coiled-coil regions are well known protein–protein interaction modules (Lupas, 1996). Indeed, the second coiled-coil domain of BRMS1 (residues 130–187) has been shown to be involved in interactions with ARID4A, which is part of the SIN3:histone deacetylase chromatin-remodelling complex (Hurst *et al.*, 2008). We have recently performed yeast two-hybrid assays and determined the participation of the N-terminal coiled coil of human BRMS1 in interactions with both cytoplasmic and nuclear proteins relevant to cancer (Rivera *et al.*, unpublished work). Structural characterization of BRMS1 can provide important information
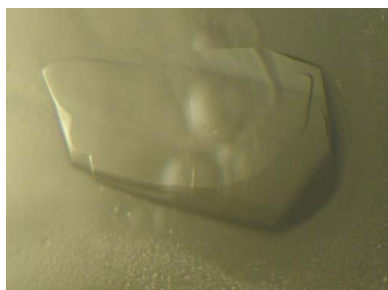
Table 1
Crystal parameters and data-processing statistics.

Values in parentheses are for the highest resolution shell.

|	
Space group	$C222_1$
Unit-cell parameters (Å)	$a = 42.6$, $b = 191.3$, $c = 71.9$
Resolution limits (Å)	95.78–2.00 (2.11–2.00)
Mosaicity (°)	0.55
Total No. of observations	146014
Unique reflections	20344
Multiplicity	7.2 (3.9)
R_{meas}†	0.055 (0.237)
R_{pim}‡	0.019 (0.119)
Mean $I/\sigma(I)$	28.2 (7.2)
Completeness (%)	99.2 (94.7)

† $R_{meas} = \sum_{hkl}[N/(N-1)]^{1/2} \sum_i |I_i(hkl) - \langle I(hkl)\rangle|/\sum_{hkl}\sum_i I_i(hkl)$, where $I_i(hkl)$ are the observed intensities, $\langle I(hkl)\rangle$ are the average intensities and N is the multiplicity of reflection hkl. ‡ $R_{p.i.m.} = \sum_{hkl}[1/(N-1)]^{1/2} \sum_i |I_i(hkl) - \langle I(hkl)\rangle|/\sum_{hkl}\sum_i I_i(hkl)$, where $I_i(hkl)$ are the observed intensities, $\langle I(hkl)\rangle$ are the average intensities and N is the multiplicity of reflection hkl.

on the molecular mechanisms involved in the antimetastatic properties of this gene.

2. Materials and methods

2.1. Protein expression and purification

The DNA fragments encoding the first coiled-coil motif of human BRMS1 spanning from Glu51 to Ser84 (BRMS1$_{51-84}$) was amplified by PCR from IMAGE consortium clone IRALp962L0425Q2. The forward primer used for PCR was GCGGGATCCGAGGACTAT-GAGCGACGCC and the reverse primer was GCCTCGAGTTAA-CTCAGTCGTTCCCTGAAC. The sequence was subcloned into a modified version of plasmid pET28 (Novagen) that allows the expression of an N-terminally 6×His-tagged SMT3 fusion protein (Mossessova & Lima, 2000). Cleavage of the 6×His tag with ULP specific protease renders a single extra serine at the N-terminus of the final construct. The inserts were verified by DNA sequencing. Plasmids were transformed into *Escherichia coli* Rosetta (DE3) cells for expression of BRMS1$_{51-84}$. Overproduction of the target protein was carried out at 310 K using 2×TY medium (16 g l^{-1} tryptone, 10 g l^{-1} yeast extract, 85 mM NaCl pH 7.2). Expression was induced by the addition of 0.5 mM isopropyl β-D-1-thiogalactopyranoside (IPTG) when the optical density at 600 nm reached a value of 0.7. Cells were harvested after 4 h and resuspended in lysis buffer (50 mM Tris–HCl
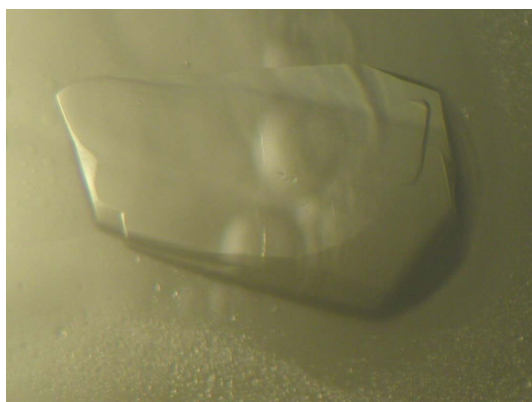
Figure 1
Crystal of BRMS1 amino-terminal coiled-coil region (residues 51–84) obtained by the hanging-drop vapour-diffusion technique. The crystal was grown using 100 mM sodium acetate pH 4.3, 200 mM ammonium sulfate and 2% PEG 4000 in the reservoir. The approximate dimensions of the crystal were 0.5 × 0.4 × 0.15 mm.

pH 7.5, 500 mM NaCl, 0.5% Tween-20) with 0.2 mM AEBSF [4-(2-aminoethyl)benzenesulfonyl fluoride hydrochloride; Sigma] as a protease inhibitor. After cell lysis by sonication and removal of cell debris by centrifugation (30 min at 20 000g), the fusion proteins were bound to 5 ml Hi-Trap Chelating columns previously loaded with nickel sulfate, washed with 50 mM Tris–HCl pH 7.5, 150 mM NaCl and eluted with 13 column volumes of a linear gradient of 0–500 mM imidazole in 50 mM Tris–HCl pH 7.5, 150 mM NaCl. The ULP specific protease was added to the eluate at 1:1000(w:w) and the mixture was dialyzed overnight (12–16 h) at 277 K against 50 mM Tris–HCl pH 7.5, 150 mM NaCl. Samples were loaded onto a second chelating column for tag removal. The flowthrough was injected onto a gel-filtration column (Superdex 75 26/60, GE Healthcare) equilibrated with 20 mM Tris pH 7.5, 50 mM NaCl and 2 mM DL-dithiothreitol (DTT). Purified protein was concentrated using Amicon Ultra Centrifugal filters of 3 kDa (UFC-800324) molecular-weight cutoff, flash-cooled under liquid nitrogen and stored at 193 K until use. The SDS–PAGE band corresponding to BRMS1$_{51-84}$ was confirmed by mass spectrometry.

2.2. Protein crystallization and X-ray data collection

For crystallization, 1 µl purified BRMS1$_{51-84}$ protein at 100–150 mg ml^{-1} (BioRad Protein Assay; reference 500-0006) in gel-filtration buffer was mixed with 1–2 µl reservoir solution (100 mM sodium acetate pH 4.3–4.5, 200 mM ammonium sulfate, 1–6% PEG 4000) and equilibrated against 0.5 ml reservoir solution in 24-well plates (Qiagen). Crystals were grown by the hanging-drop vapour-diffusion method at 298 K, appearing in 3 d to one week and reaching their maximum size in a month. Crystals were cryoprotected using Paratone-N (Hampton Research), mounted on cryoloops and flashed-cooled at 130 K under a cryogenic nitrogen stream.

Two data sets, a low-resolution pass (95.8–5.0 Å) and a high-resolution pass (57.5–2.0 Å), were collected on ID14-1 at the ESRF, Grenoble, France (Table 1) using a wavelength of 0.934 Å and an ADSC Quantum Q210 CCD detector. The crystal-to-detector distances were 551.82 and 229.63 mm for the low- and high-resolution data sets, respectively. Data reduction was performed using the programs *MOSFLM* v.7.0.2 and *SCALA* v.3.3.2 from the *CCP*4 program suite (Collaborative Computational Project, Number 4, 1994).

3. Results and discussion

Human BRMS1 N-terminal coiled-coil region (residues 51–84) was successfully expressed in *E. coli* Rosetta cells and purified using metal-chelate affinity chromatography followed by size-exclusion chromatography. As the Superdex 75 26/60 column had been calibrated with proteins covering the range 12.4–6.5 kDa (amongst others), the elution volume of the peptide in the gel filtration of 211.9 ml was estimated to correspond to a molecular weight of around 9 kDa, suggesting the formation of a dimer in solution. The crystals grew to typical dimensions of 0.3 × 0.2 × 0.1 mm. Several crystals grew to a larger size of 0.5 × 0.4 × 0.15 mm (Fig. 1). Initial crystals were obtained in the presence of 2 mM DTT. Crystals appeared in 4–5 weeks under these conditions. The absence of reducing agents shortened the time required for crystal formation to 1–2 weeks without any apparent loss in crystal size or quality and DTT was therefore removed from subsequent crystallization experiments. The crystals cracked or lost diffraction power when cryoprotectants differing from Paratone-N were used either in soaking or

crystallization communications
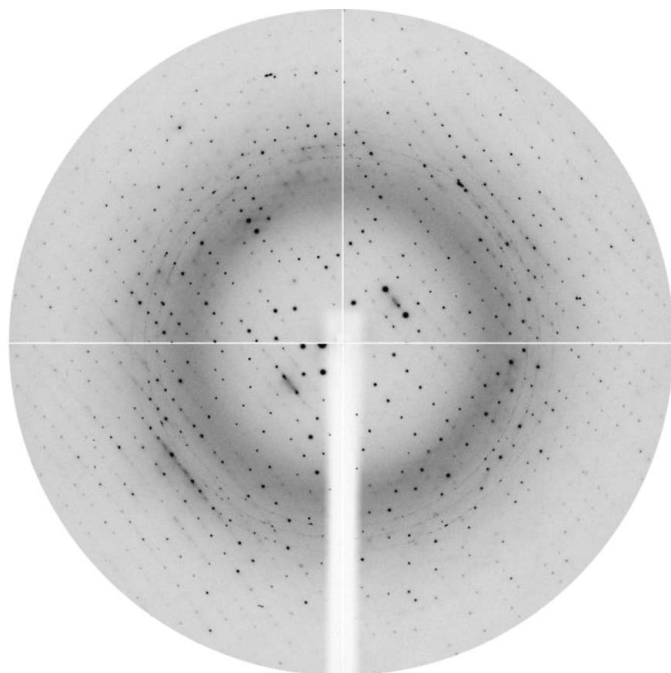
Figure 2
Example of the diffraction pattern of the BRMS1$_{51-84}$ crystal with a 1.0° rotation oscillation. The edge of the detector corresponds to a resolution of 2.0 Å.

cocrystallization experiments. The cryoprotectants tested included glycerol, MPD, ethylene glycol and PEG 4000.

Diffraction data were collected to 2.0 Å resolution (Fig. 2). The data statistics of the X-ray diffraction experiments are shown in Table 1. Systematic extinctions confirmed that the crystals belong to space group $C222_1$. The unit-cell parameters are $a = 42.6$, $b = 191.3$, $c = 71.9$ Å.

The number of molecules in the asymmetric unit could vary between six and eight, with estimated Matthews coefficients of 2.8 and 2.1 Å^3 Da^{-1}, respectively, corresponding to a solvent content of between 56 and 41%. The self-rotation function does not allow unambiguous distinction between six or eight molecules in the asymmetric unit. Molecular-replacement techniques are unlikely to provide initial phasing since no similar structures are available and the number of molecules in the asymmetric unit is relatively large. An average model using several coiled-coil structures was also unsuccessful and a heavy-atom derivative search has therefore been initiated.

This is the first crystallization report of a fragment of human BRMS1 or any of its orthologues.

References

Cicek, M., Fukuyama, R., Welch, D. R., Sizemore, N. & Casey, G. (2005). *Cancer Res.* **65**, 3586–3595.
Collaborative Computational Project, Number 4 (1994). *Acta Cryst.* D**50**, 760–763.
DeWald, D. B., Torabinejad, J., Samant, R. S., Johnston, D., Erin, N., Shope, J. C., Xie, Y. & Welch, D. R. (2005). *Cancer Res.* **65**, 713–717.
Gupta, G. P. & Massague, J. (2006). *Cell*, **127**, 679–695.
Hurst, D. R., Mehta, A., Moore, B. P., Phadke, P. A., Meehan, W. J., Accavitti, M. A., Shevde, L. A., Hopper, J. E., Xie, Y., Welch, D. R. & Samant, R. S. (2006). *Biochem. Biophys. Res. Commun.* **348**, 1429–1435.
Hurst, D. R., Xie, Y., Vaidya, K. S., Mehta, A., Moore, B. P., Accavitti-Loper, M. A., Samant, R. S., Saxena, R., Silveira, A. C. & Welch, D. R. (2008). *J. Biol. Chem.* **283**, 7438–7444.
Liu, Y., Smith, P. W. & Jones, D. R. (2006). *Mol. Cell Biol.* **26**, 8683–8696.
Lupas, A. (1996). *Trends Biochem. Sci.* **21**, 375–382.
Mossessova, E. & Lima, C. D. (2000). *Mol. Cell*, **5**, 865–876.
Nikolaev, A. Y., Papanikolaou, N. A., Li, M., Qin, J. & Gu, W. (2004). *Biochem. Biophys. Res. Commun.* **323**, 1216–1222.
Phadke, P. A., Vaidya, K. S., Nash, K. T., Hurst, D. R. & Welch, D. R. (2008). *Am. J. Pathol.* **172**, 809–817.
Rivera, J., Megias, D. & Bravo, J. (2007). *J. Proteome Res.* **6**, 4006–4018.
Saunders, M. M., Seraj, M. J., Li, Z., Zhou, Z., Winter, C. R., Welch, D. R. & Donahue, H. J. (2001). *Cancer Res.* **61**, 1765–1767.